Supporting Information for "A subjective Bayesian framework for synthesizing deep uncertainties in climate risk management"

James Doss-Gollin[1], Klaus Keller[2]

[1]Department of Civil and Environmental Engineering, Rice University

[2]Thayer School of Engineering, Dartmouth College

This document contains supplementary methods, figures, and tables for the paper "A subjective Bayesian framework for synthesizing deep uncertainties in climate risk management" by James Doss-Gollin and Klaus Keller.

S1. Supplemental methods

S1.1. Statistical distributions

To avoid ambiguity, we define here some statistical distributions used in the main text. Except where otherwise indicated, we follow the default notation of the Distributions.jl Julia package (Besançon et al., 2021).

S1.1.1. Generalized Extreme Value distribution

We parameterize the generalized extreme value (GEV) distribution as

$$f(x|\mu,\sigma,\xi) = \begin{cases} \frac{1}{\sigma}\left[1+\left(\frac{x-\mu}{\sigma}\right)\xi\right]^{-1/\xi-1} \exp\left\{-\left[1+\left(\frac{x-\mu}{\sigma}\right)\xi\right]^{-1/\xi}\right\}, & \xi \neq 0 \\ \frac{1}{\sigma}\exp\left\{-\frac{x-\mu}{\sigma}\right\}\exp\left\{-\exp\left[-\frac{x-\mu}{\sigma}\right]\right\}, & \xi = 0. \end{cases} \tag{S1}$$

Corresponding author: J. Doss-Gollin, Department of Civil and Environmental Engineering, Rice University, Houston, TX, USA (jdossgollin@rice.edu)

S1.1.2. Inverse Gamma distribution

Parameterizing the Inverse Gamma distribution as

$$f(x|\alpha,\theta) = \frac{\theta^\alpha x^{-(\alpha+1)}}{\Gamma(\alpha)} e^{-\frac{\theta}{x}}, \quad x > 0, \tag{S2}$$

the parameters α and θ can be computed from the desired mean μ and standard deviation σ as

$$\begin{aligned} \alpha &= 2 + \frac{\mu^2}{\sigma^2} \\ \theta &= \mu(\alpha - 1). \end{aligned} \tag{S3}$$

S1.1.3. Gamma distribution

We parameterize the Gamma distribution as

$$f(x|\alpha,\theta) = \frac{x^{\alpha-1} e^{-x/\theta}}{\Gamma(\alpha)\theta^\alpha}, \quad x > 0. \tag{S4}$$

S1.1.4. Plotting position

The plotting position used in fig. 5 is the Weibull ("empirical") plotting position

$$^{r}/_{N+1} \tag{S5}$$

where N is the sample size and r is the order of the N observations ($r = 1$ is the largest, $r = N$ is the smallest).

S1.2. Algorithm to estimate expected damages

As discussed in section 3.3, we use a Monte Carlo integration to estimate expected damages D as a function of house elevation $h = h_0 + \delta h$ and mean relative sea level (MSL), $y(t)$. Specifically, for $m = 1, \ldots, M$:

1. draw a sample from the posterior distribution of storm surge (see eq. (2)) $\{\mu_m, \sigma_n, \xi_m\}$

2. simulate a single storm surge from this stationary GEV distribution and add the mean sea level to get total flood depth y_m^{sim}

3. calculate the flood damages for this draw by plugging the annual maximum flood depth relative to the house,$h - y'(t)$, into the deterministic HAZUS depth-damage relationship, storing this as the mth damage.

We then estimate expected annual damages as the sample mean of the M estimates.

S1.3. Surrogate model for expected annual damages

Evaluating expected annual damages for each of J simulations of sea level rise (SLR), each of N draws from the posterior distribution of storm surge, and each of T time steps for K models requires $N \times J \times T \times K$ simulations. In our model, we have $T = 70$, $N = 10\,000$, $J = 179\,232$, hence exhaustive sampling may be prohibitive.

Noticing that this function depends only on the elevation of the house relative to MSL, we develop a simple emulator for expected annual damages given this difference: $\hat{D}(h - \overline{y})$. To do this, we precompute expected annual damage for all height differences in 0.25 ft increments from −30 ft to 30 ft and fit a piecewise linear interpolation to this data. We use $K = 1 \times 10^6$ samples to fit this emulator for each of the 241 increments. This model is shown in fig. S2. Once this interpolation has been precomputed, calculating expected annual damage for a particular year only requires evaluating a piecewise linear function.

References

Besançon, M., Papamarkou, T., Anthoff, D., Arslan, A., Byrne, S., Lin, D., & Pearson, J. (2021). Distributions.jl: Definition and Modeling of Probability Distributions in the JuliaStats Ecosystem. *Journal of Statistical Software*, *98*(16). doi: 10.18637/

jss.v098.i16

Coles, S. G., & Tawn, J. A. (1996). A Bayesian analysis of extreme rainfall data. *Journal of the Royal Statistical Society: Series C (Applied Statistics)*, *45*(4), 463–478. doi: 10.2307/2986068

Gelman, A., Carlin, J. B., Stern, H. S., & Rubin, D. B. (2014). *Bayesian Data Analysis* (Third ed.). Chapman & Hall/CRC Boca Raton, FL, USA.

Gelman, A., Vehtari, A., Simpson, D., Margossian, C. C., Carpenter, B., Yao, Y., … Modrák, M. (2020, November). Bayesian workflow. *arXiv:2011.01808 [stat]*. doi: 10.48550/arXiv.2011.01808

Geyer, C. J. (1992). Practical Markov Chain Monte Carlo. *Statistical Science*, *7*(4), 473–483.

Huizinga, J., & Szewczyk, W. (2016). *Global flood depth-damage functions: Methodology and the database with guidelines.* LU: Publications Office of the European Union.

Johnson, D. R., Fischbach, J. R., & Ortiz, D. S. (2013, August). Estimating surge-based flood risk with the Coastal Louisiana Risk Assessment model. *Journal of Coastal Research*, *67*(sp1), 109–126. doi: 10.2112/si_67_8

McElreath, R. (2020). *Statistical rethinking: A Bayesian course with examples in R and Stan* (Second edition. ed.). Boca Raton ;: CRC Press, Taylor & Francis Group.

Zarekarizi, M., Srikrishnan, V., & Keller, K. (2020, October). Neglecting uncertainties biases house-elevation decisions to manage riverine flood risks. *Nature Communications*, *11*(1), 5361. doi: 10.1038/s41467-020-19188-9

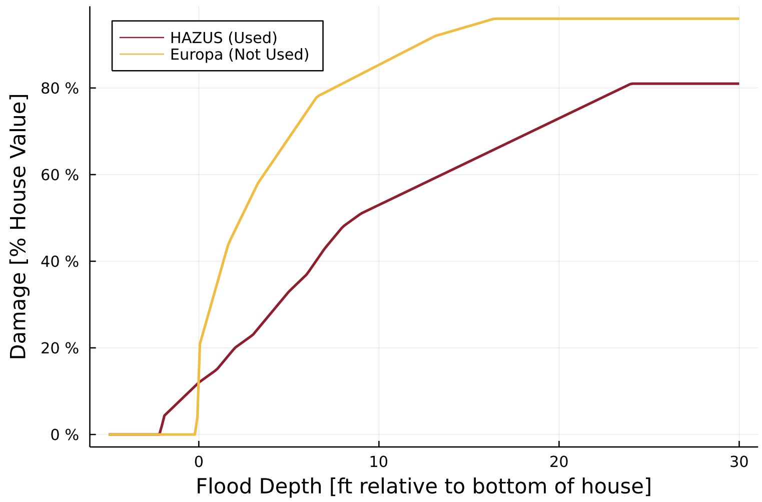

Figure S1. Depth-damage relationship. Following Zarekarizi et al. (2020), we use the HAZUS depth-damage curves. Since results are sensitive to choice of depth-damage equation, we illustrate (for comparison only) the "Europa" depth-damage relationship developed by the Joint Research Center (JRC) of the European Commission's science and knowledge service (Huizinga & Szewczyk, 2016).

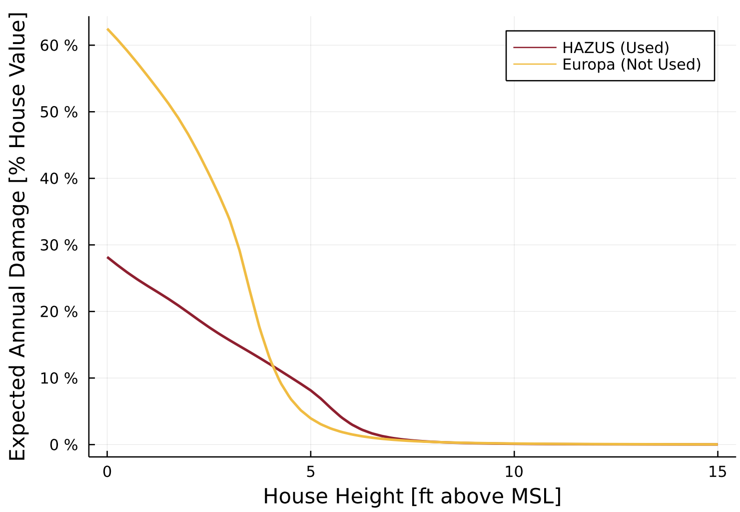

Figure S2. As discussed in section 3.3, we model expected annual damages (eq. 3) as a function of the house's elevation relative to MSL. Damages (y axis) are shown as a percentage of house value.

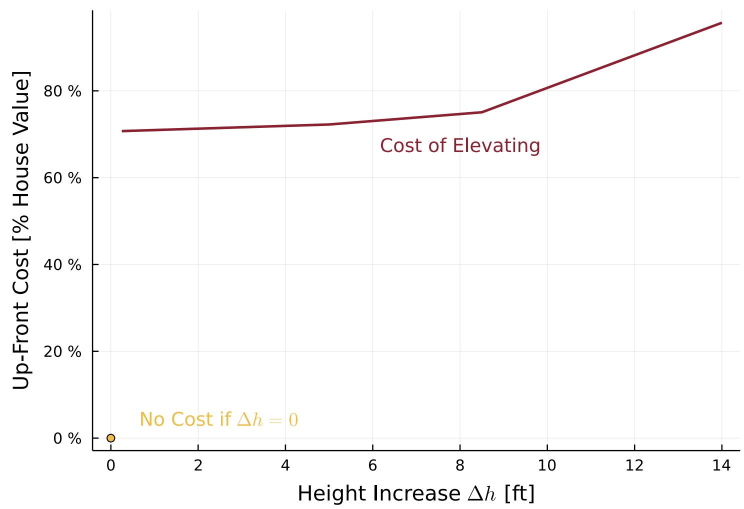

Figure S3. Following Zarekarizi et al. (2020), we model the cost of elevating a single-family house by interpolating estimates from the Coastal Louisiana Risk Assessment Model (Johnson et al., 2013). According to this model, the unit cost of elevating a house by 3-7, 7-10, and 10-14 feet is \$82.50, \$86.25, and \$103.75 per square foot, respectively, with a \$20 745 initial cost. Values are sensitive to house floor area and structural value; see table 1.

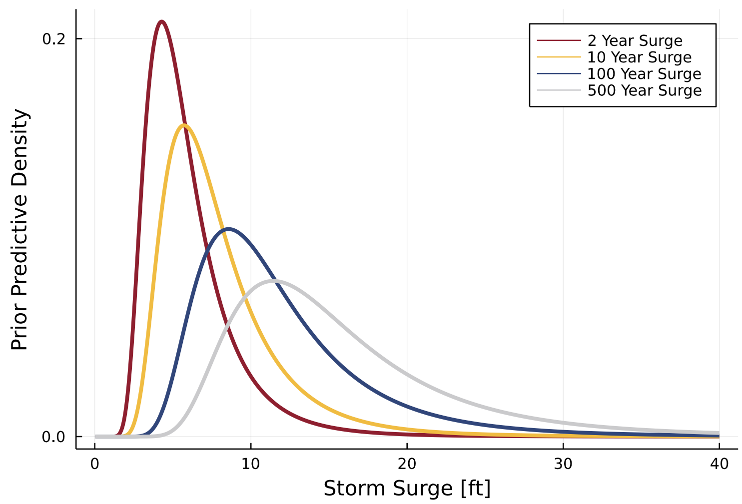

Figure S4. Prior distributions for annual maximum storm surge. Rather than apply a prior over model parameters directly, we apply a weakly informative prior over quantiles of the resulting distribution (that is, over a function of the model parameters) following Coles and Tawn (1996). See section 3.2 for details. For the 2, 10, 100, and 500 year events we apply Inverse Gamma distributions, with means 4 ft, 6 ft, 10 ft and 15 ft and standard deviations 1.5 ft, 1.75 ft, 2.25 ft and 2.75 ft, respectively.

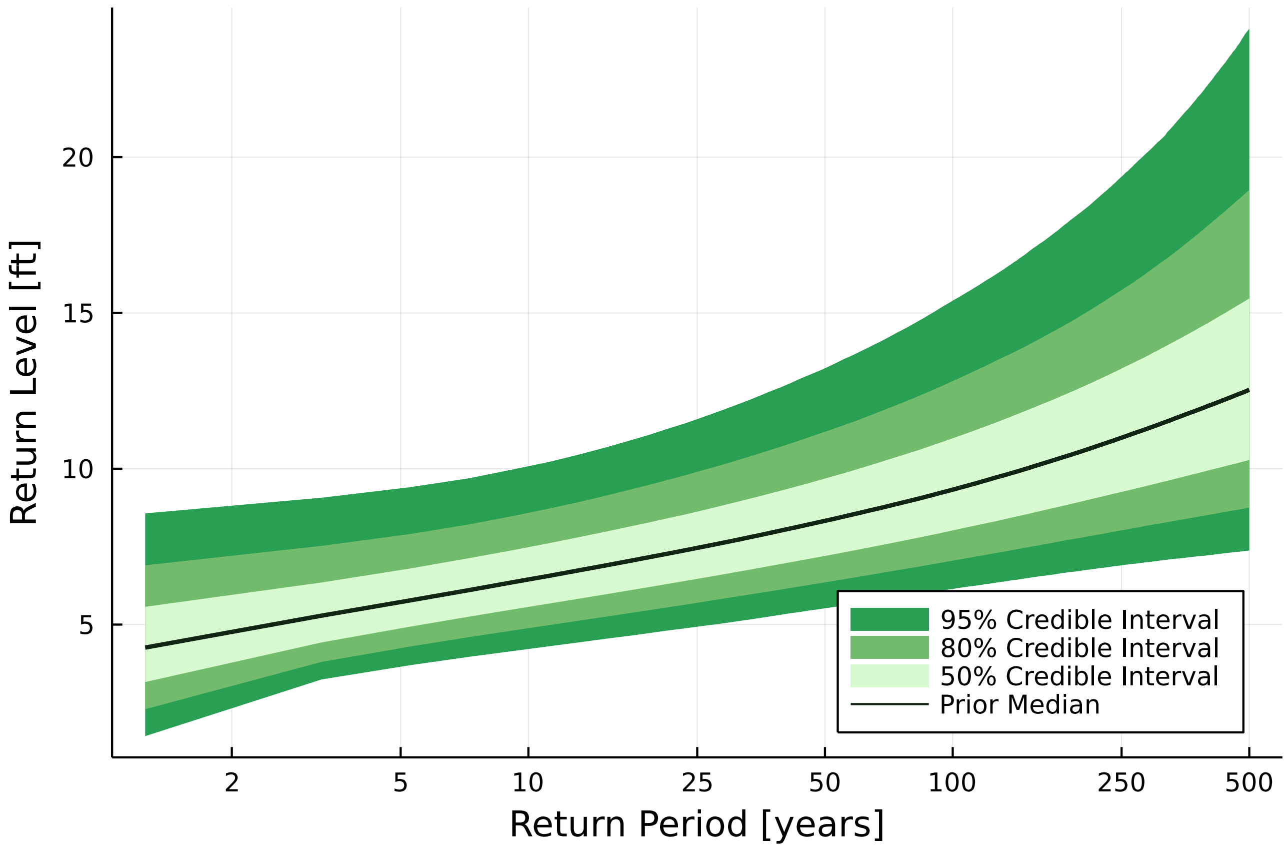

Figure S5. Implicit prior over storm surge represents large uncertainty but is consistent with basic physical reasoning (see section 3.2). The prior median (blue line) and uncertainty quantiles (shading) of the return period for different return levels of storm surge at Sewells Point, VA using prior predictive sampling (Gelman et al., 2020). This illustrates the weakly informative prior information (section 3.2) used in the analysis. These weakly informative priors were selected to be consistent with basic physical principles (*e.g.*, storm surges most years are > 2 ft but rarely exceed 20 ft).

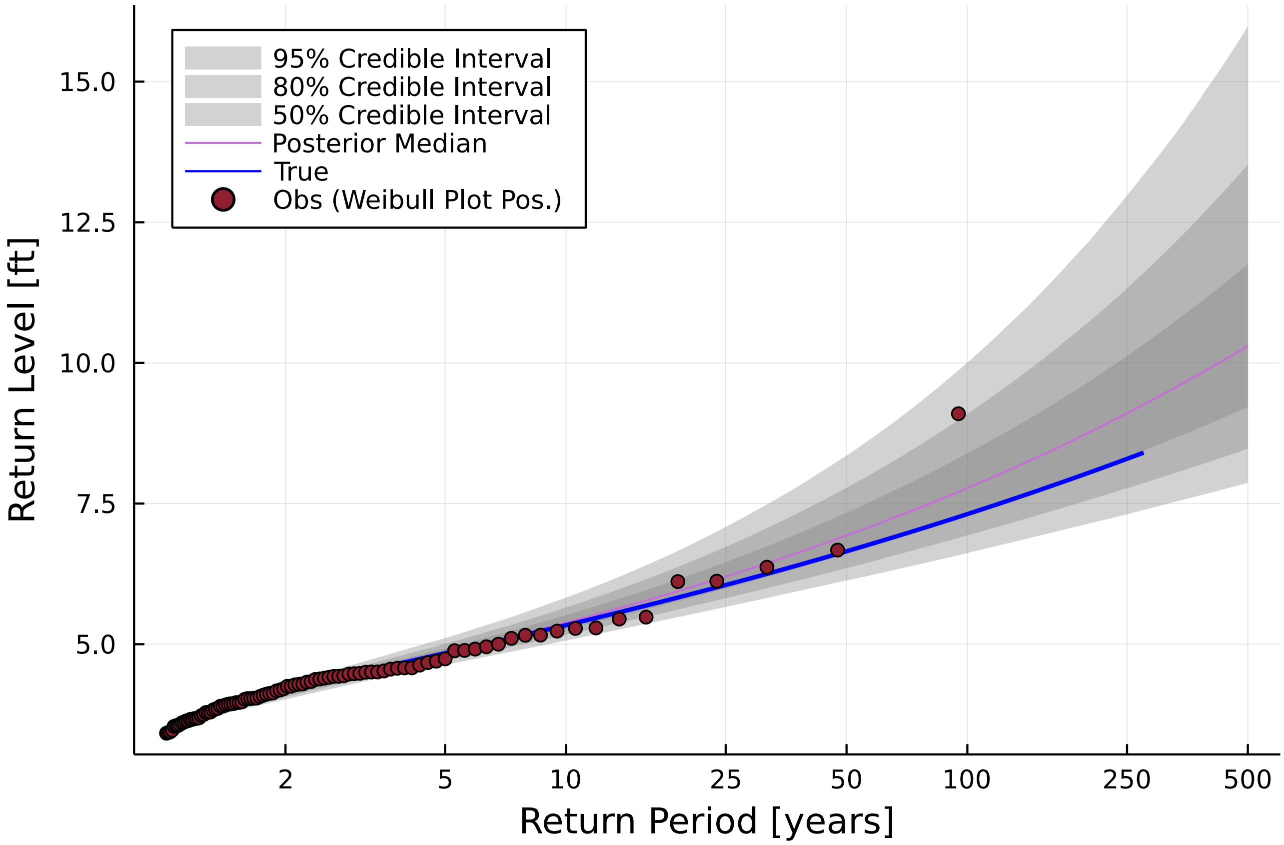

Figure S6. Synthetic data experiment as a positive control test for the GEV model of storm surge. A synthetic record (dots) was sampled from a GEV distribution with location, scale, and shape parameters of 4, 0.5, and 0.15, respectively. These samples were used to fit the Bayesian GEV model described in section 3.2; the gray shading indicates the 50, 80, and 95% posterior confidence intervals. The blue line shows the true quantiles of the (known) GEV distribution. By random chance the sample maximum has a true return period of $\gg 250$ years, which increases the upper confidence interval of the estimated return probabilities, but the true value is nevertheless within the 50% posterior confidence interval. This experiment yields similar results for alternative values of the known GEV distribution, and for different random seeds (not shown).

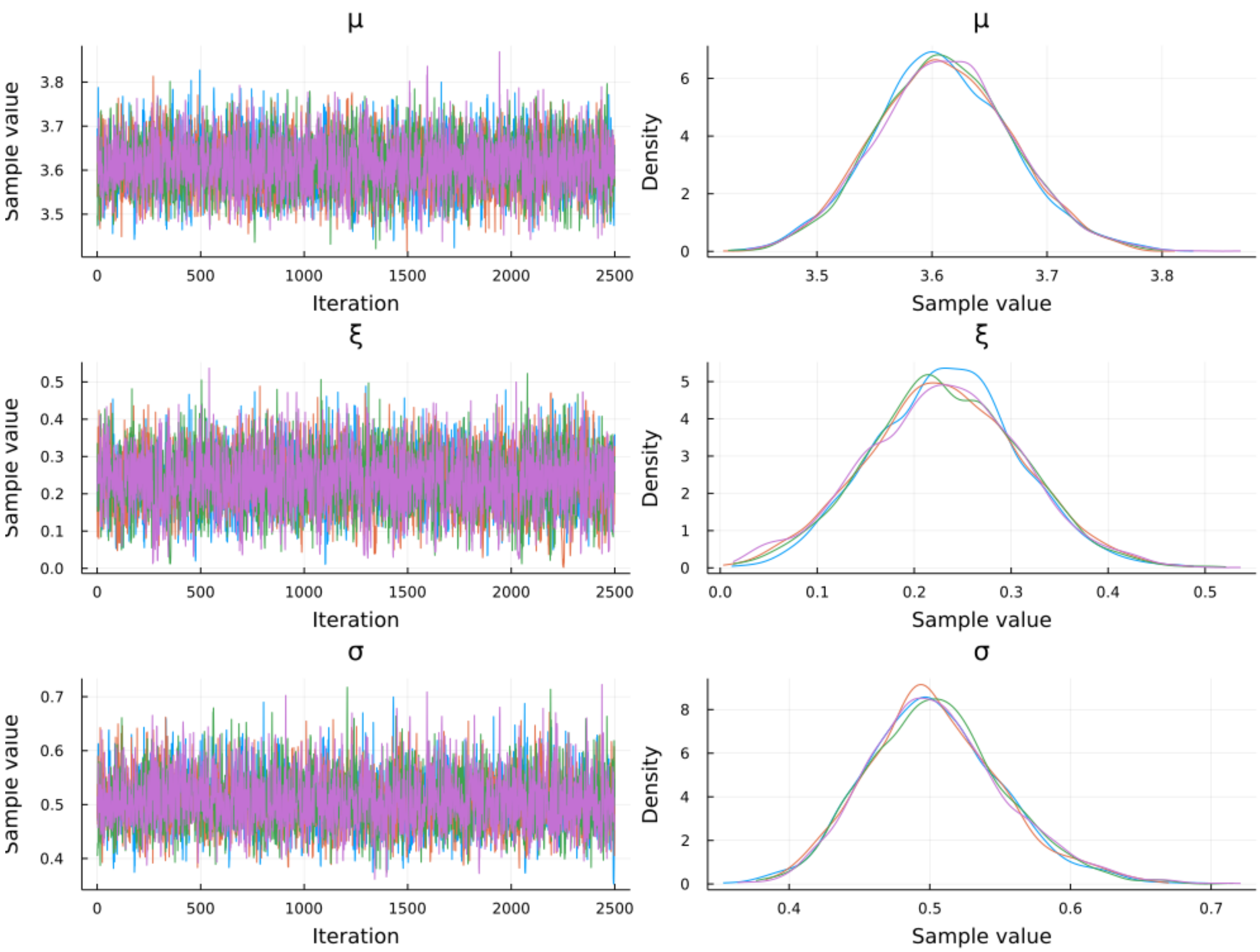

Figure S7. Markov chain diagnostic plots for posterior draws from the storm surge model. We draw 10 000 samples by running four chains of 3500 iterations each and discarding the first 1000. The mixing of the chains is consistent with, though does not guarantee, convergence.

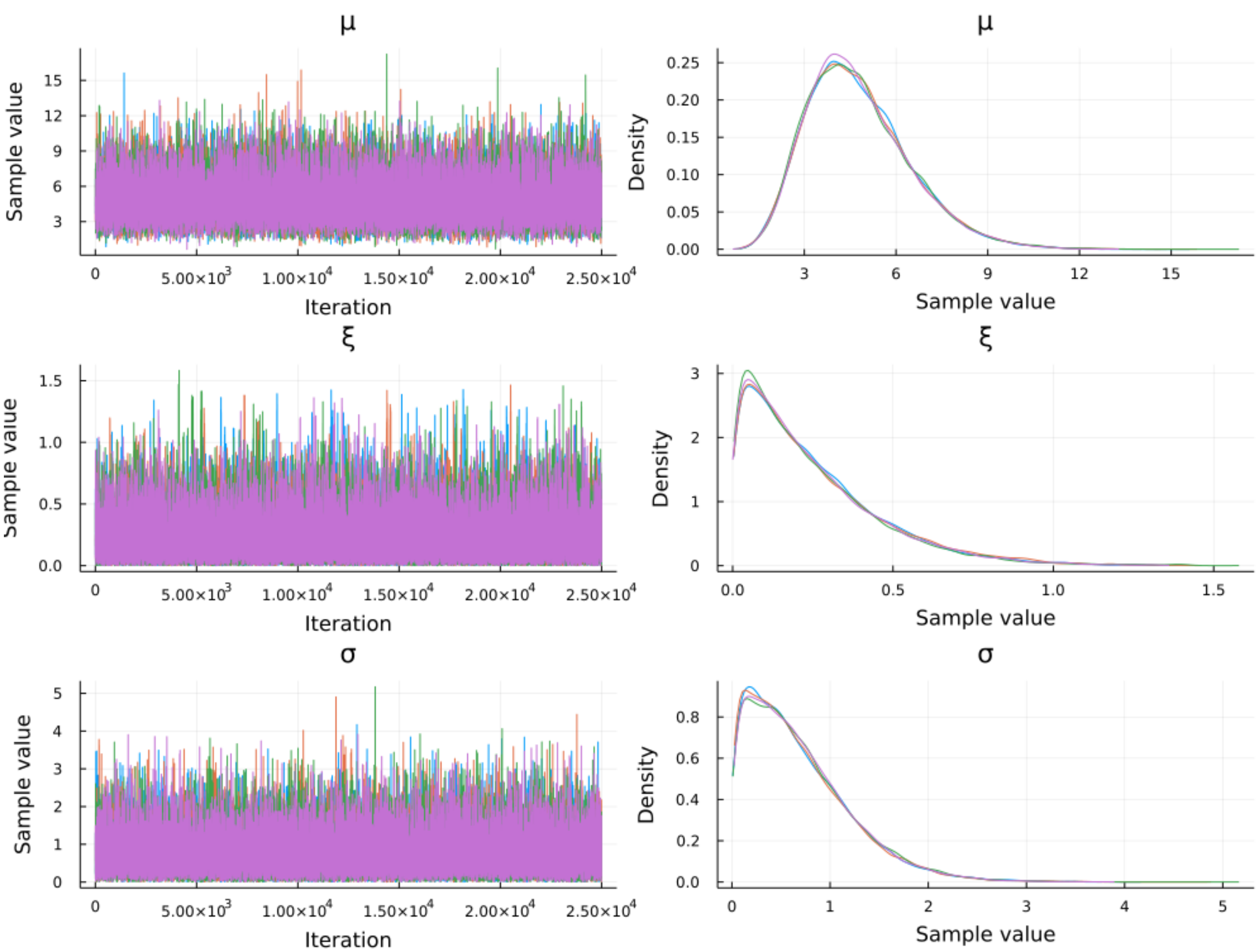

Figure S8. As fig. S7, but for draws from the prior distribution.

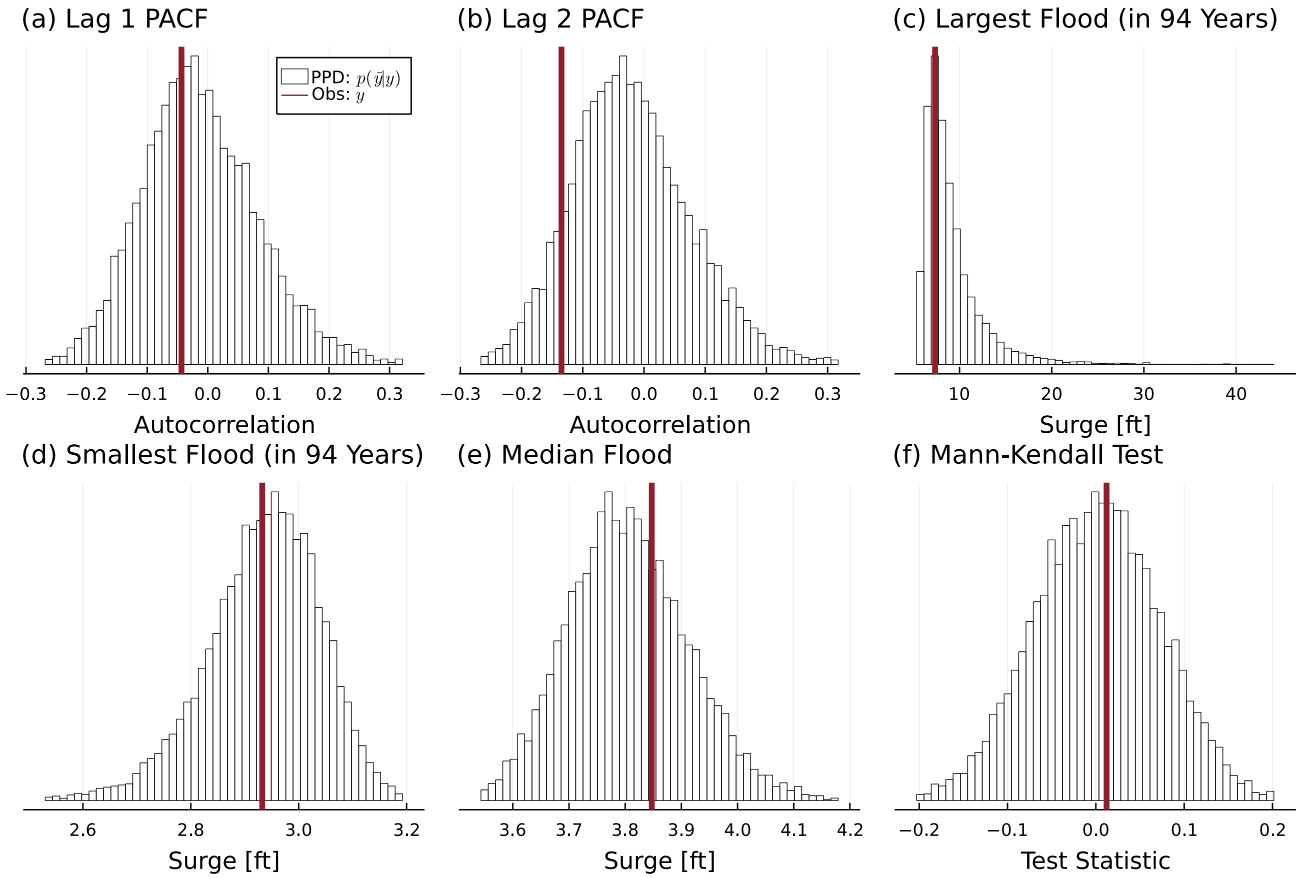

Figure S9. Posterior predictive checks for the stationary GEV storm surge model (section 3.2). Each panel shows a different test statistic: partial autocorrelation at lags 1 and 2; sample maximum; sample minimum; sample median; and Mann-Kendall trend test statistic. The histograms show the distribution of each test statistic from the posterior predictive distribution. Orange lines show the test statistic's value in the observed data. Observed values near the mode of the posterior predictive distribution are consistent with, but do not guarantee, a good fit. For further discussion of posterior predictive checks, see Chapter 6 of Gelman et al. (2014).

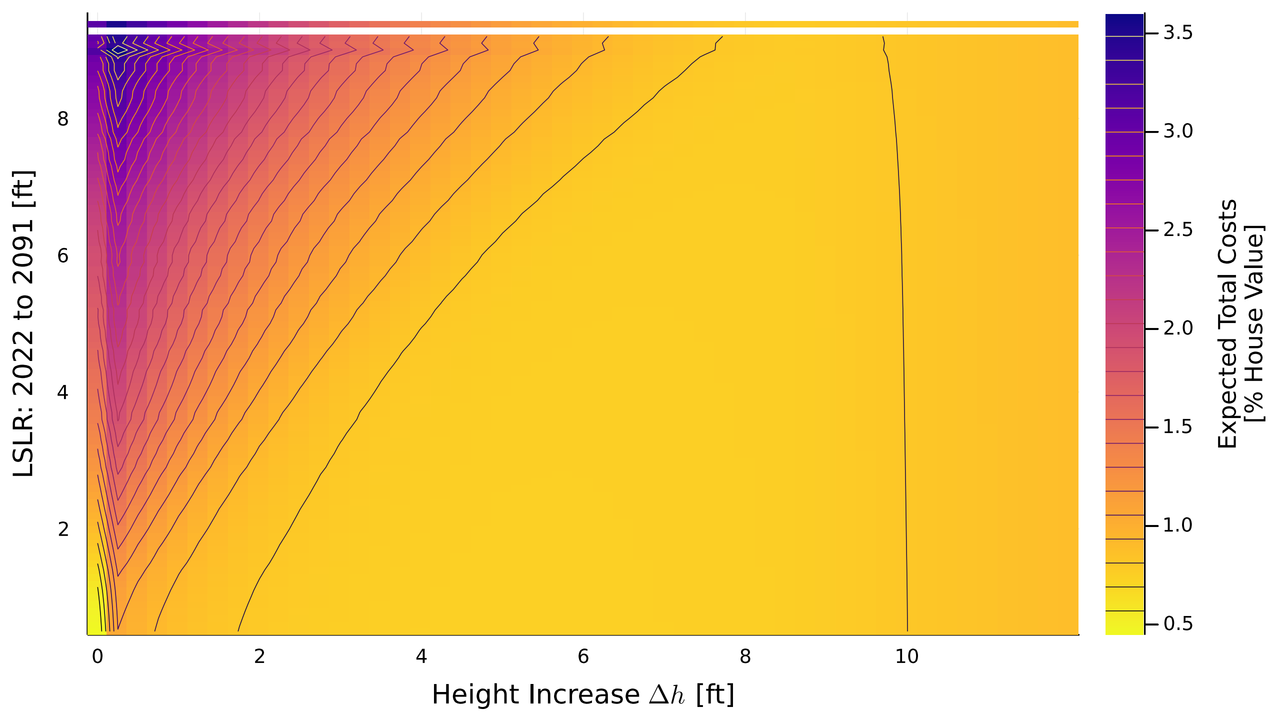

Figure S10. Expected total lifetime cost (damages plus up-front cost) as a function of SLR over the house lifetime and height increase Δh. Initial house elevation is fixed to 1 ft below the BFE. Expectations were computed for discrete values of Δh (x axis) by discretizing SOWs (y axis), then taking the sample mean over each grid cell.

Table S1. Diagnostic statistics for the Hamiltonian Monte Carlo sampling for the storm surge posterior draws. Statistics include the mean and standard deviation of each parameter, the naive standard error and Monte Carlo standard error (which measure uncertainty in the mean), the effective sample size, $\hat{R}$ diagnostic, and effective samples per second, which describes sampling speed. The naive standard error (SE) returns the standard error of the mean. The Monte Carlo standard error (MCSE) is calculated using the initial monotone sequence estimator (Geyer, 1992, pp. 473-483). The effective sample size (ESS) is a crude estimate of the number of independent samples and is calculated following Geyer (1992, pp. 473-483). The $\hat{R}$ is an indicator of the convergence of the Markov chains to the target distribution; a value $\hat{R}$ value close to one is consistent with, though does not guarantee, convergence (McElreath, 2020). For additional details see the `MCMCDiagnosticTools` package documentation.

Parameter	Mean	Stdev.	Naive SE	MCSE	ESS	$\hat{R}$
μ	3.610	0.059	0.001	0.001	4922.462	1.001
ξ	0.231	0.079	0.001	0.001	4609.415	1.001
σ	0.504	0.049	0.000	0.001	4547.881	1.001

Table S2. As table S1 but for draws from the prior distribution.

Parameter	Mean	Stdev.	Naive SE	MCSE	ESS	$\hat{R}$
μ	4.774	1.702	0.005	0.011	26657.405	1.000
ξ	0.246	0.215	0.001	0.002	11238.145	1.000
σ	0.682	0.531	0.002	0.004	24720.263	1.000